UCSF
UC San Francisco Previously Published Works

## Title

Using Flow Cytometry to Compare the Dynamics of Photoreceptor Outer Segment Phagocytosis in iPS-Derived RPE CellsPhagocytosis in iPS-Derived RPE Cells

## Permalink

https://escholarship.org/uc/item/8q59w13w

## Journal

Investigative Ophthalmology & Visual Science, 53(10)

## ISSN

0146-0404

## Authors

Westenskow, Peter D
Moreno, Stacey K
Krohne, Tim U
et al.

## Publication Date

2012-09-14

## DOI

10.1167/iovs.12-9721

Peer reviewed

eScholarship.org Powered by the California Digital Library
University of California

Translational

# Using Flow Cytometry to Compare the Dynamics of Photoreceptor Outer Segment Phagocytosis in iPS-Derived RPE Cells

*Peter D. Westenskow,[1] Stacey K. Moreno,[1] Tim U. Krohne,[1] Toshihide Kurihara,[1] Saiyong Zhu,[2] Zhen-ning Zhang,[3] Tongbiao Zhao,[3] Yang Xu,[3] Sheng Ding,[2] and Martin Friedlander[1]*

**Purpose.** Retinal pigment epithelium (RPE) autologous grafts can be readily derived from induced pluripotent stem (iPS) cells. It is critical to stringently characterize iPS-RPE using standardized and quantifiable methods to be confident that they are safe and adequate replacements for diseased RPE before utilizing them in clinical settings. One important and required function is that the iPS-RPE phagocytose photoreceptor outer segments (POS).

**Methods.** We developed a flow cytometry-based assay to monitor binding and internalization of FITC labeled POS by ARPE-19, human fetal RPE (hfRPE), and two types of iPS-RPE. Expression and density of $\alpha_v\beta_5$ integrin, CD36, and MerTK receptors, which are required for phagocytosis, were compared.

**Results.** Trypsinization of treated RPE cells results in the release of bound POS. The number of freed POS, the percentage of cells that internalized POS, the brightness of the FITC signal from the cells, and the surface density of the phagocytosis receptors on single RPE cells were measured using flow cytometry. These assays reveal that receptor density is dynamic during differentiation and this can affect the binding and internalization dynamics of the RPE cells. Highly differentiated iPS-RPE phagocytose POS more efficiently than hfRPE.

**Conclusions.** Caution should be exercised to not use RPE grafts until demonstrating that they are fully functional. The density of the phagocytosis receptors is dynamic and may be used as a predictor for how well the iPS-RPE cells will function in vivo. The phagocytosis dynamics observed between iPS-RPE and primary RPE is very encouraging and adds to mounting evidence that iPS-RPE may be a viable replacement for dysfunctional or dying RPE in human patients. (*Invest Ophthalmol Vis Sci.* 2012;53:6282–6290) DOI:10.1167/iovs.12-9721

The retinal pigment epithelium (RPE) is a multifunctional ocular tissue that encapsulates the neural retina and is required for photoreceptor function and vision.[1] The basal surfaces of RPE cells are separated from the choriocapillaris, the primary blood supply for photoreceptors, by Bruch's membrane and regulate transport of ions, nutrients, and water to and from the blood supply to the subretinal space. RPE cells secrete many important signaling molecules including VEGF and PEDF and also re-isomerize retinals, the light sensitive visual pigments, to maintain visual cycling. On their apical surfaces, RPE cells extend long apical processes that wrap around the tips of rod and cone photoreceptors. From this position they are able to phagocytose the outer segments of photoreceptors that are routinely damaged by light. In fact, photoreceptor and RPE cells are so codependent that loss or dysfunction of either results in secondary retinal degeneration, as in some cases of age-related macular degeneration (AMD) the leading cause of blindness in the elderly.[2,3] Failure to phagocytose POS in humans and rodents is itself sufficient to induce rapid and profound retinal degeneration.[4–6]

Induced pluripotent stem cells (iPSCs) can be generated from somatic cells.[7,8] RPE can be readily derived from iPSCs[9–13] and encouraging results from several independent groups, including our own,[14] have shown that implantation of stem cell–derived RPE cells in rodent models of RPE-mediated retinal degeneration successfully mediates anatomical and functional rescue of photoreceptors.[10,15,16] Work remains, however, to more stringently characterize RPE cells derived from human embryonic stem cells (hES) and human induced pluripotent stem cells (hiPS) to confirm that stem cell derived RPE will function adequately in compromised retinas. Some of these assays, including those to measure the dynamics of POS phagocytosis, are neither standardized nor sufficiently quantitative. Conventional methods to measure the rates of phagocytosis involve challenging monolayers of RPE cells with POS labeled with fluorescent biomarkers. After washing and fixing the cells, the POS that are bound to the cell surfaces or that are internalized can be detected using a fluorescence microscope, counted, and recorded to yield the total number of POS present. When this assay is employed over multiple time points, the dynamics of POS binding and internalization can be compared in vitro in a semiquantitative fashion utilizing Trypan blue, which quenches the fluorescence of bound, but not internalized, POS. The sample is then treated with Trypan blue and counted again. The total number of POS minus the

From the [1]Department of Cell Biology, The Scripps Research Institute, La Jolla, California; the [2]Gladstone Institute of Cardiovascular Disease, University of California, San Francisco (UCSF), San Francisco, California; and the [3]Section of Molecular Biology, Division of Biological Sciences, University of California, San Diego (UCSD), La Jolla, California.

Supported by grants from the California Institute for Regenerative Medicine (TRI-01219), a Ruth Kirschstein Fellowship of the National Eye Institute (EY021416 [PDW]), a fellowship from the Manpei Suzuki Diabetes Foundation and The Japan Society for the Promotion of Science (JSPS) Postdoctoral Fellowships for Research Abroad (TK), and the National Eye Institute (EY11254 [MF]).

Submitted for publication February 17, 2012; revised June 12, 2012; accepted July 20, 2012.

Disclosure: **P.D. Westenskow**, None; **S.K. Moreno**, None; **T.U. Krohne**, None; **T. Kurihara**, None; **S. Zhu**, None; **Z.N. Zhang**, None; **T. Zhao**, None; **Y. Xu**, None; **S. Ding**, None; **M. Friedlander**, None

Corresponding author: Martin Friedlander, Department of Cell Biology, The Scripps Research Institute, MB28, 10550 North Torrey Pines Road, La Jolla, CA 92037; friedlan@scripps.edu.



Investigative Ophthalmology & Visual Science, September 2012, Vol. 53, No. 10
Copyright 2012 The Association for Research in Vision and Ophthalmology, Inc.

internalized number of POS (post Trypan count) gives the number of bound POS.

The long-term goal of our research is to generate patient matched autologous RPE grafts for AMD patients from iPS cells. We choose to use iPS reprogrammed with viral delivered octamer-binding transcription factor 4 (OCT4) and small molecules (1F-iPS) or with episomal vectors (EiPS-RPE) for several reasons: (1) to minimize possible risks of oncogenesis if the transcription factors become reactivated, (2) to alleviate potential regulatory concerns regarding cells reprogrammed with multiple randomly integrating viral delivered transcription factors, and (3) since 1F-iPS–RPE reprogramming is efficient and can be used to generate RPE cells that strongly resemble hfRPE based on anatomical, functional, proteomic, and metabolomic assays.[14] Robust characterization of the EiPS-RPE is underway. 1F-iPS–RPE phagocytose POS in vitro (as determined using conventional assays) and function in vivo to phagocytose debris in the subretinal space of RCS rats.[14] To monitor iPS-RPE more accurately, we decided to develop a more quantitative technique to directly compare phagocytosis dynamics between primary RPE and iPS-RPE, since RPE phagocytosis is such an important function.

To provide more substantial evidence that iPS-RPE cells phagocytose POS at comparable rates and share similar binding and internalization kinetics as primary human RPE cells, we developed a flow cytometry–based assay to determine how effectively iPS-RPE phagocytose isolated POS in vitro. In this study we compare the dynamics of four human RPE cell types: human fetal RPE (hfRPE), RPE derived from 1F-iPS-RPE,[17] EiPS-RPE,[18] and ARPE-19, an immortalized RPE cell line utilized for many of the founding phagocytosis studies.

The mechanisms of photoreceptor outer segment phagocytosis have been well studied. While there is still an active debate over the specific ligands and receptors involved in RPE phagocytosis, several cell surface receptors, including $\alpha_v\beta_5$ integrins,[19–21] CD36[22], and MerTK[6] have been implicated. $\alpha_v\beta_5$ integrin is most likely the primary binding receptor.[19,20] In β5 integrin mutant mice dramatic deficits in retinal function are observed based on electroretinography experiments.[23] CD36 receptors, which reportedly are required and sufficient in vitro for POS internalization, appear to function independently of $\alpha_v\beta_5$ integrins,[24] and retinal degeneration is observed in CD36 mutant mice.[25] MerTK is responsible for POS internalization and is the defective gene in the RCS rat, which exhibits profound retinal degeneration and lacks the ability to phagocytose outer segments.[4,6] Humans with MerTK mutations also display profound rod and cone dystrophies.[5] Other receptors that regulate RPE phagocytosis have been identified including CD81[26] and the mannose receptor,[27] however, the exact functions and importance of these receptors remains to be determined. To determine how receptor density corresponds with phagocytosis, we utilized an over expression assay to monitor receptor density, binding, and internalization dynamics at different stages of RPE differentiation using flow cytometry. We report here that receptor density is critical, and an altered balance of receptor densities dramatically affects the dynamics of RPE cells to phagocytose POS.

## Materials and Methods

### Maintenance of Cell Lines

For our studies we used ARPE-19 cells (ATCC, Manassas, VA), primary hfRPE cells (Lonza, Walkersville, MD) and iPS-RPE. We generated iPS using viral delivered OCT4 and small molecules as previously reported,[17] or with episomal vectors also as previously reported,[18] and differentiated the iPS to iPS-RPE using published techniques.[15] We thoroughly characterized the 1F-iPS–RPE and showed that they strongly resemble hfRPE in multiple assays, and showed that they function in vivo to phagocytose debris from the subretinal space of RCS rats and mediate anatomical and functional rescue of photoreceptors.[14] 1F-iPS-RPE, hfRPE, and ARPE-19 cell lines were expanded and maintained as previously described.[14] The same protocols were utilized to generate EiPS-RPE. Great care was taken to make sure that after seeding new cultures, sufficient time was allowed for the cells to stabilize (generally 2-3 weeks). For 1F-iPS–RPE and hfRPE, cultures were only used that were pigmented, displayed classic cobblestone morphologies, and formed domes (indicating vectorial transport of ions and water).

For the over expression studies, ARPE-19 cells were transfected using a Cell Line Nucleofector Kit V kit and Amaxa nucleofector technology using program X-01 (Lonza). 1,000,000 cells were mixed with 2 μg of plasmid DNA encoding either pMax-GFP (Lonza), CD36-GFP (Addgene plasmid 21,853; Addgene, Cambridge, MA),[28] MerTK (Addgene plasmid 14,998; Addgene),[29] or 1μg $\alpha_v$ integrin and 1μg $\beta_5$ integrin (from David Cheresh, UCSD). After nucleofection, the cells remained in the cuvette for 10 minutes before seeding into one well of a 6-well plate. Transfection efficiencies (generally 80%–90%) were monitored by GFP fluorescence. Assays were performed 3 days post transfection.

### Porcine POS Isolation and Labeling

Fresh pig eyes were obtained from Sierra for Medical Sciences (Los Angeles, CA). POS were isolated and FITC labeled as reported previously.[14] POS were examined using electron microscopy to verify that intact outer segments were collected (See Supplementary Material and Supplementary Fig. S1, http://www.iovs.org/lookup/suppl/doi:10.1167/iovs.12-9721/-/DCSupplemental). POS were aliquoted and stored at −80°C until the day of the assay. The total micrograms of protein were quantified using Bradford Assays with a SmartSpec Plus spectrophotometer (Bio-Rad, Hercules, CA).

### POS Phagocytosis Assays

To develop the assay, cells were treated with varying concentrations of photoreceptor outer segments from 1 to 10 ug/cm$^2$ for 30 minutes to 7 hours. Finally, 4 ug/cm$^2$ POS (the optimal concentration) was added for 30 minutes, 2 hours, or 5 hours. Untreated cells were used to obtain baseline fluorescence. Cells were treated with FITC labeled outer segments as described above and incubated at 37°C. Cells were rinsed with 1X Dulbecco's PBS (with Calcium; Invitrogen) and treated with trypsin (TrypLE; Invitrogen) for 5 to 8 minutes to detach cells and release bound outer segments. DMEM/F12 (Invitrogen) containing 2% FBS (Invitrogen) was added to neutralize the trypsin and cells were transferred to falcon tubes (BD). Samples were diluted 1:1 with FACS staining buffer (BD) containing DRAQ5 (1:2500; Cell Signaling). Cells were labeled with DRAQ5 before analysis to distinguish cells from debris and outer segments. Samples were analyzed immediately on a FACSCanto flow cytometer (BD). Cells were gated based on DRAQ5 labeling, and 5000 events were collected per sample. Data were analyzed using FlowJo software (version 8.8.6; Tree Star, Inc., Ashland, OR).

### Receptor Expression

To examine receptor density, cells were seeded on UpCell plates with temperature sensitive adhesion matrices (Thermo Fisher Scientific, Pittsburg, PA). Prior to staining, the cells were released by moving the plate from 37°C to room temperature for 5 to 10 minutes and gently scrapping with a cell scraper, TPP, Trasadingen, Switzerland). Multiple wells were combined into a single tube. Cells were pelleted by centrifugation and resuspended in FACS staining buffer to a concentration of 5,000,000 cells per milliliter. 1,000,000 cells (200 ul) were transferred to falcon tubes containing one of the following antibodies

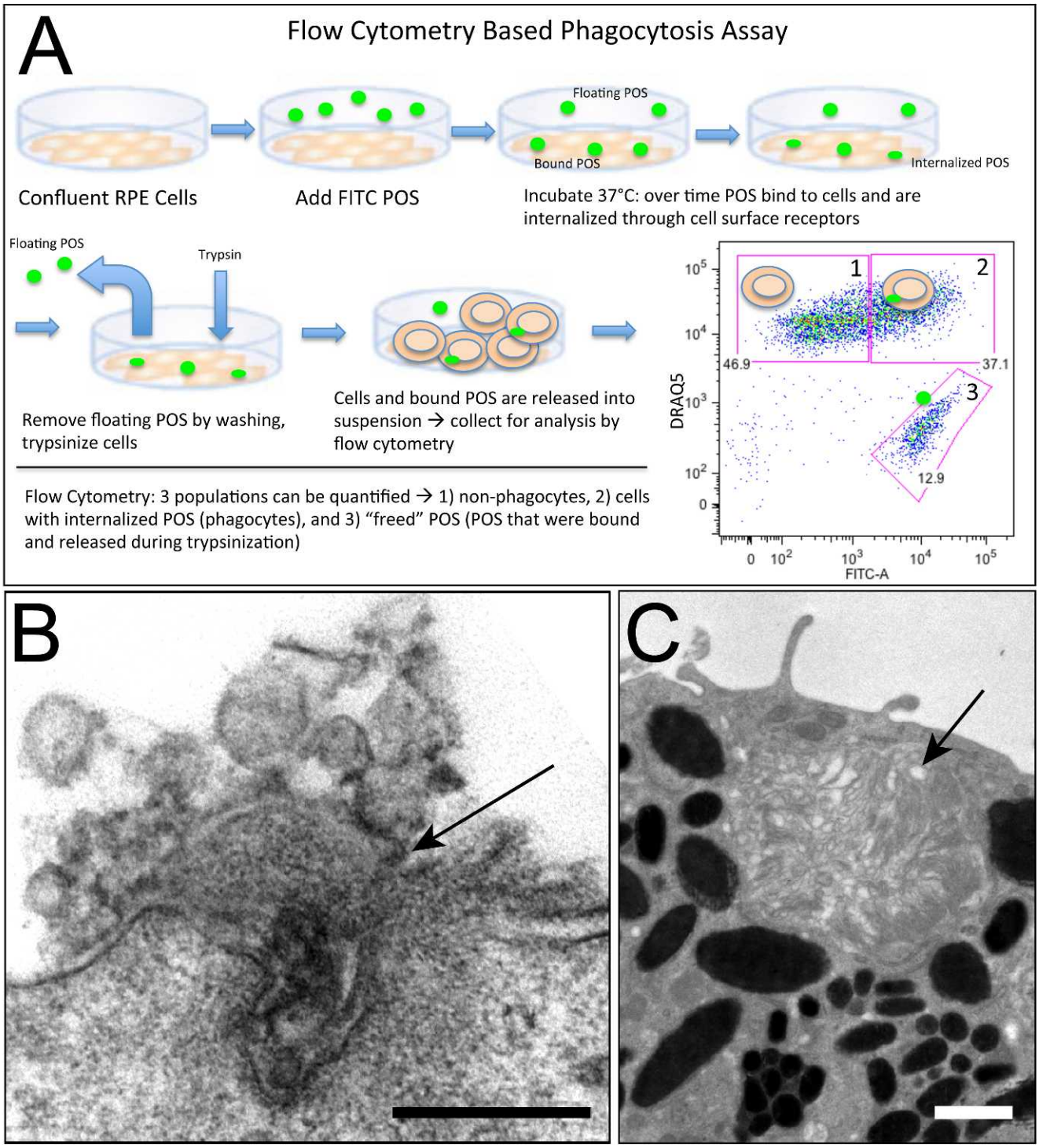


**Figure 1.** (**A**) Schematic illustrating the flow cytometry–based phagocytosis assay. (**B**) Electron micrograph showing bound POS at the surface of a murine primary RPE cell (*arrow*); *scale bar* = 200 nm. (**C**) Image showing internalized POS in murine RPE (*arrow*); *scale bar* = 1 μm.

or isotype controls; all concentrations used were based on the manufacturer's recommendations: P1F6 (anti-αvβ5 integrin) PE Millipore (Billerica, MA) MAB1961H: 10 ul/test; PE Mouse IgG1 Millipore CBL600P:10 ul/test; anti-CD36 FITC SCT10426: 20 ul/test; FITC Mouse IgG1 SCT10310: 20 ul/test; anti-MerTK PE R&D Systems (Minneapolis, MN) FAB8912P:10 ul/test; PE Mouse IgG1 R&D IC002P: 10 ul/test. Samples were incubated at room temperature, in the dark for 30 minutes. Cells were washed one time with staining buffer, pelleted by centrifugation and resuspended in 1% paraformaldehyde. Samples were fixed for 5 minutes and washed. Cells were suspended in 300 ul staining buffer containing DRAQ5 (1:5000) for analysis. Analysis was done on a FACSCanto (BD).

## Electron Microscopy

Mice were killed in adherence to the ARVO Statement for the Use of Animals in Ophthalmic and Vision Research and perfused with 0.9% saline followed by perfusion fixation with 4% paraformaldehyde, 1.5% gluteraldehyde, and 0.02% picric acid in 0.1 M cacodylate buffer and,

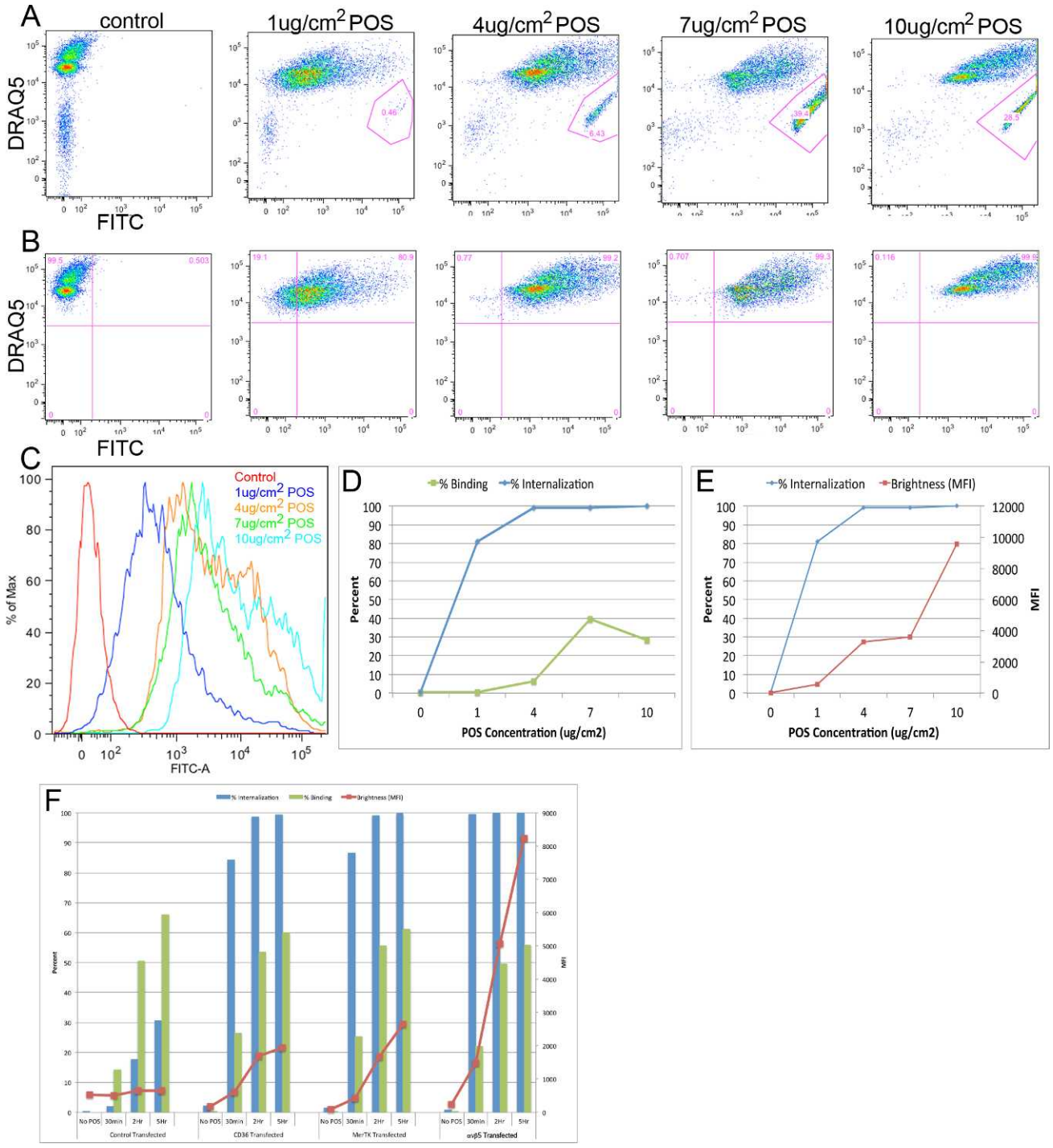


**Figure 2.** Establishment of the flow cytometry–based assay in ARPE-19 cells. (**A**) Maximum phagocytosis is reached with 4 ug/cm$^2$ outer segments at 5 hours. (**B**) Gating the freed POS reveals that binding is increased at 7 ug/cm$^2$ but plateaus at higher concentrations (red gates). Gating the phagocytes in the same sample reveals that the brightness of the phagocytes increases with increasing amounts of outer segments indicating continued internalization. (**C**) Quantification (histogram) of data shown in Panel **A**. (**D**–**E**) Quantification of data shown in Panels **A** and **B**. Both the percentage of cells internalizing POS (*blue*; *left*: *y*-axis) and MFI (*red*; *right*: *y*-axis) representing amount internalized is shown in (**E**). (**F**) αvβ5 integrin, CD36, and MerTK over expression dramatically alters the phagocytic dynamics of RPE cells compared with ARPE-19 transfected with GFP. The percentage of cells binding and internalizing POS (*bars*; *left*: *y*-axis) and MFI (*dots/line*; *right*: *y*-axis) representing the amount of POS internalized is shown.

following dissection of the eye including halving the eye close to the optic nerve, continued prolonged immersion fixation at 4°C. The tissues were then buffer washed, post fixed in 1% osmium tetroxide, and subsequently dehydrated in graded ethanol series, transitioned in propylene oxide and embedded in LX112 resin (Ladd Research Industries, Williston, VT). Thick cross sections close to the optic nerve (2 μm) were cut, mounted on glass slides, and stained in toluidine blue for general assessment in the light microscope. Subsequently, 70 nm thin sections were cut with a diamond knife (Diatome, Hatfield, PA), mounted on copper slot grids precoated with parlodion, and then stained with uranyl acetate and lead citrate for examination and documentation on an electron microscope (Philips CM100; FEI, Hillsbrough, OR) at 80 kV.

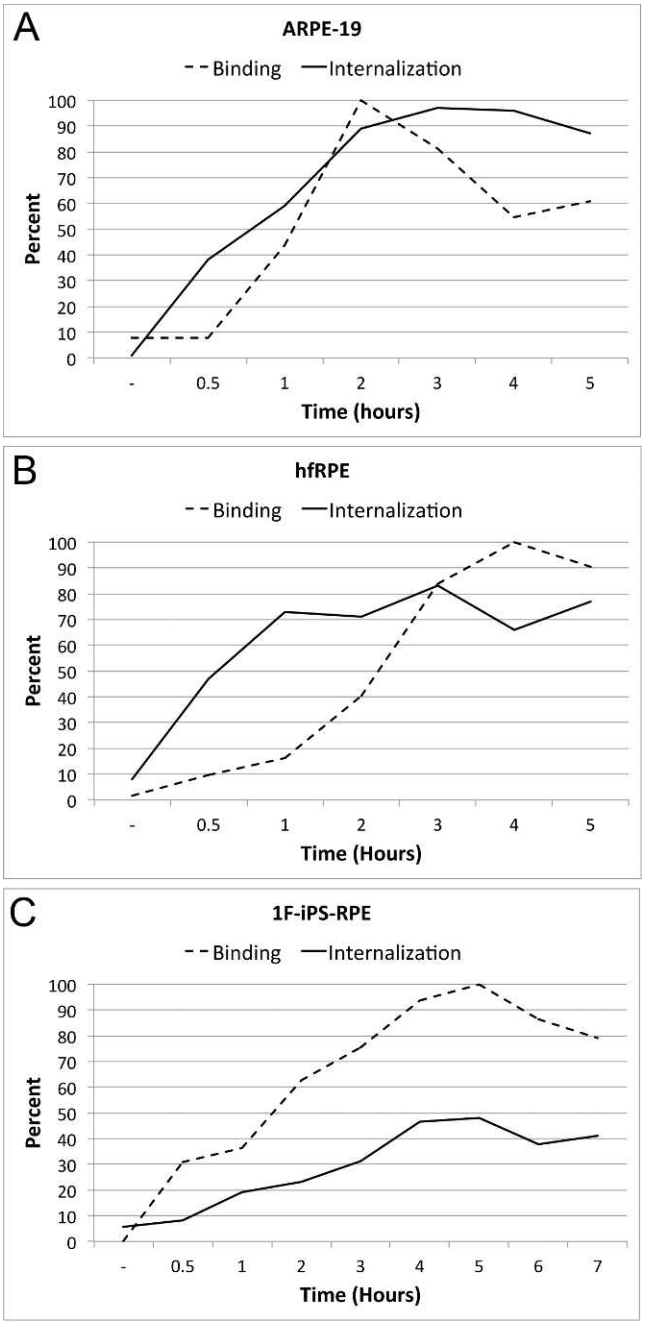


**Figure 3.** Binding and internalization time course comparison. (**A**) ARPE19 reaches maximum binding at 2 hours and internalization at 3 hours. For all the graphs the percent binding (*dashed line*) and the percent internalization (phagocytosis; *solid line*) are shown. (**B**) hfRPE are slightly slower than ARPE19 reaching maximum binding at 3 hours and internalization at 3 to 5 hours. (**C**) iPSC-derived RPE reach both maximum binding and internalization at 4 to 5 hours. Overall binding and internalization levels are lower for both hfRPE and 1F-iPSC as compared with ARPE19.

Images were documented using a camera (Megaview III ccd; Olympus Soft Imaging Solutions, Lakewood, CO).

## Results

In this study, we report that trypsinization of RPE cells challenged with isolated POS results in a release of bound species. To verify that all FITC fluorescence measured by flow cytometry is in fact due to internalized POS, samples were analyzed, treated with Trypan blue, and analyzed again. No change in percent positive or mean fluorescence intensity of phagocytes was observed. All fluorescence of the POS alone population was completely quenched (See Supplementary Material and Supplementary Fig. S2, http://www.iovs.org/lookup/suppl/doi:10.1167/iovs.12-9721/-/DCSupplemental). When analyzed using flow cytometry, therefore, we can detect three populations: a set of cells that has not internalized POS, a set of cells that has internalized POS (and median fluorescence intensity [MFI] or brightness values representing amount of POS ingested), and POS that have attached to the cells but were released by proteolysis, referred to throughout the text as "freed" POS (see Fig. 1A for a schematic depiction of the assay). When analyzed cumulatively, we provide a more complete depiction of the amount of POS bound by RPE cells and the amount ingested than that obtained using conventional methods. Utilizing flow cytometry, we have developed a quick, higher throughput method of analysis that provides data on both parameters of phagocytosis: binding and internalization. Previous studies using flow cytometry were limited to measures of internalization only[30] or require pH specific dyes.[31,32] (See Figs. 1B, 1C for electron micrographs of bound and internalized POS).

We then challenged confluent RPE cultures with FITC-labeled porcine POS for 5 hours, trypsinized the cells, and then labeled them with DRAQ5, a fluorescent nuclear marker that labels all cells prior to analyses. Using this method we can easily distinguish cells and isolated POS (See Supplementary Material and Supplementary Fig. S3, http://www.iovs.org/lookup/suppl/doi:10.1167/iovs.12-9721/-/DCSupplemental). The percentage of cells phagocytosing POS and those that are not can be quantified by gating signals from unfed cells (based on background readings in the FITC channel). This percentage increases to 76.9% after POS challenge indicating active RPE phagocytosis (See Supplementary Material and Supplementary Fig. S3, http://www.iovs.org/lookup/suppl/doi:10.1167/iovs.12-9721/-/DCSupplemental). After comparing both techniques in parallel, we determined that analyzing freed POS after trypsinization was just as effective and much simpler than performing the extra Trypan blue quenching step.

To establish the assay and to determine an optimal concentration of POS to use in our assays, we exposed ARPE-19 cells to POS for 5 hours to elicit maximal internalization. At 1 $\mu g/cm^2$ nearly all POS available were internalized by 5 hours (Figs. 2A–C). At 4 $\mu g/cm^2$, 100% of the cells had internalized some amount of POS by 5 hours, but a small amount was bound but not internalized (6.4%), suggesting that this is an appropriate dose for future experiments (Fig. 2A). When more POS is made available, RPE continued to phagocytose in a linear manner, as detected by increasing MFI (Fig. 2D, 2E). At higher concentrations (7–10 $\mu g/cm^2$) the binding sites become saturated and the percentage of freed POS plateaus (Fig. 2C).

Since the initial steps of phagocytosis are controlled by cell surface receptors, we decided to alter the densities of the receptors to examine the effects and to validate that changes in the dynamics of phagocytosis could be determined using the flow cytometry-based assay. A low phagocytic percentage of control ARPE-19 cells nucleofected with GFP was observed (likely since only a few days passed after trypsinization), however, those transfected with CD36, or MerTK began phagocytosing at normal levels and $\alpha_v\beta_5$ integrin transfected cells began phagocytosing above normal levels (Fig. 2F). In fact, the MFI brightness values in $\alpha_v\beta_5$ integrin transfected cells were greater than 8-fold higher than in untransfected cells and 4- and 2.5-fold above CD36 or MerTK transfected cells, respectively (Fig. 2F). From these assays, we determined that

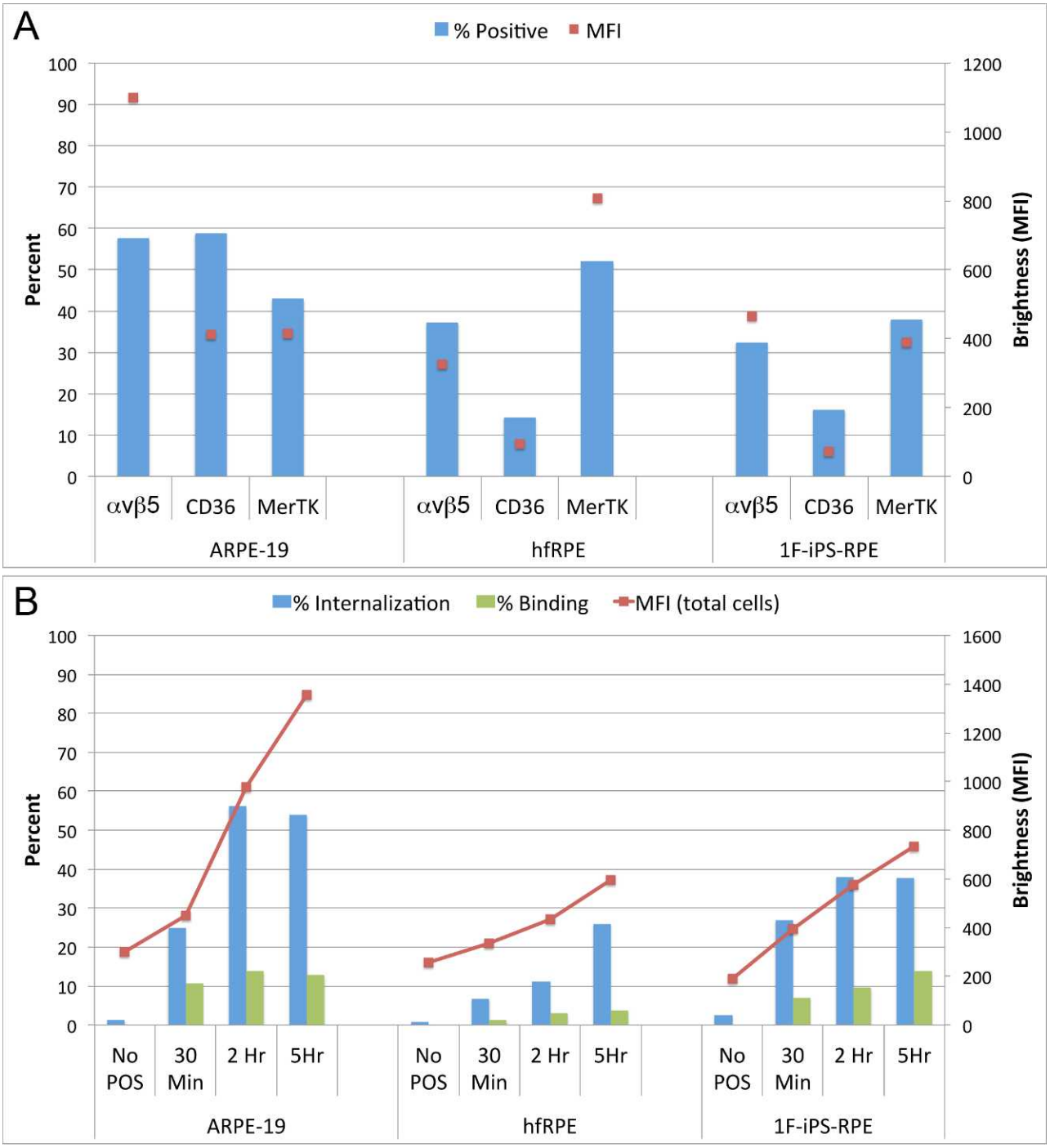


**Figure 4.** **(A–B)** Levels of receptor expression on each cell type correlate with their ability to bind and internalize outer segments. Panel **A** shows percentage of both cells positive (*bars*; *left*: *y*-axis) for each receptor as well as overall brightness of the sample (*dots*; *right*: *y*-axis). Increased brightness indicates increased receptor density. Panel **B** shows levels of phagocytosis as measured by flow cytometry at 30 minutes, 2 hours, and 5 hours post treatment. Percent internalization (*blue bars*; *left*: *y*-axis), percent binding (*green bars*; *left*: *y*-axis), and MFI (*red dots/lines*; *right*: *y*-axis) representing the amount of POS internalized is shown.

inducing remodeling of the phagocytosis surface receptors can modulate the dynamics of binding and internalization, and these effects can be monitored using flow cytometry–based techniques.

After determining that the assay was valid, we next examined the dynamics of RPE phagocytosis over time in iPS-RPE, hfRPE, and ARPE-19. Previous studies show that maximal binding is achieved after 2 hours and maximal internalization occurs after 5 hours.[19] When exposed to 4 μg/cm$^2$ POS, we also observe maximal binding (percent binding) at 2 hours but maximal internalization occurs after as early as 3 hours (Fig. 3A). For comparison, we examined hfRPE and 1F-iPS–RPE treated with the same concentration of POS and at the same time points. hfRPE are slightly slower than ARPE-19 and reach maximal binding at 3 hours and internalization at 3 to 5 hours (Fig. 3B). 1F-iPS–RPE reach both maximum binding and

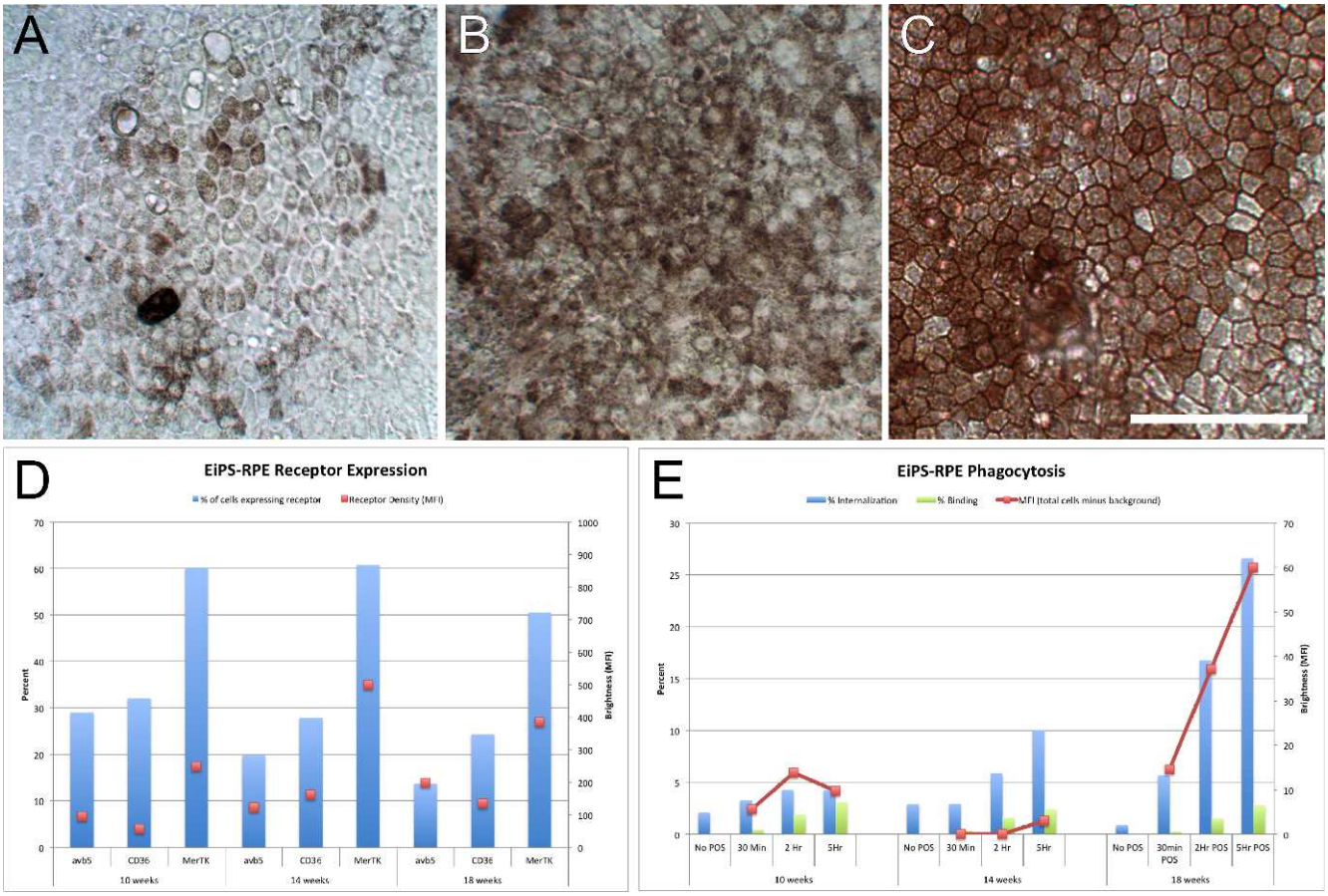


**Figure 5.** The status of surface receptor density of phagocytosis receptors and binding and internalization kinetics during RPE differentiation in EiPS-RPE is dynamic. (**A–C**) Images of EiPS-RPE after 10 weeks of directed differentiation (**A**), 14 weeks (**B**), and 18 weeks (**C**); *scale bar* = 50 μm. The percentage of cells (*bars*; *left*: *y*-axis) expressing $\alpha_v\beta_5$ integrin, CD36, and MerTK, and MFI (*dots*; *right*: *y*-axis) representing receptor densities are shown at the same time points (**D**). The percentage of cells binding and internalizing POS (*left*: *y*-axis) and MFI (*right*: *y*-axis) representing amount of POS internalized are shown at the same time points of EiPS-RPE differentiation.

internalization at 4 to 5 hours (Fig. 3C). Overall, binding and internalization is lower for both hfRPE and 1F-iPS–RPE as compared with ARPE-19 (Figs. 3A–C).

We hypothesized that the variation observed in RPE phagocytosis between different human cell types could be due to divergent phagocytosis receptor densities of $\alpha_v\beta_5$ integrin, CD36, and MerTK receptors. To test this theory we labeled the cells after release from plates coated with temperature sensitive adhesion matrices with fluorescently conjugated antibodies, and quantified the percentage of single cells expressing the receptors at levels above background fluorescence. Receptor density can be compared by examining MFI brightness values. Using this technique, we can quantify the expression of the receptors on the surface of 10,000+ single cells per experiment. In ARPE-19 cells, in which the percentage of binding and phagocytosis is highest, $\alpha_v\beta_5$ integrin, CD36, and MerTK all are detected in relatively 40% to 60% of cells. $\alpha_v\beta_5$ integrin receptor density is very high (> 2-fold higher) as compared with either hfRPE or 1F-iPS–RPE (Fig. 4A). In comparison, very distinct patterns in hfRPE and 1F-iPS–RPE cells were observed along with different binding and internalization dynamics. The phagocytosis dynamics in 1F-iPS–RPE and hfRPE cells are more similar to one another, however (Fig. 4A). When directly compared, hfRPE and 1F-iPS–RPE have similar expression patterns of $\alpha_v\beta_5$ integrins, although the receptor density in 1F-iPS–RPE is higher (Fig. 4A). The percentage of cells expressing CD36 and receptor density on the individual cells, however, is nearly identical. Conversely, hfRPE express higher levels of MerTK (percentage of positive cells and intrinsic densities; Fig. 4A).

Various RPE cells (seeded on the same day and treated in exactly the same manner) were challenged as those examined above with 4 μg/cm$^2$ POS for 30 minutes, 2 and 5 hours and were compared with naïve cells (Fig. 4B). The results of these analyses show that ARPE-19 cells display the highest percentage of internalization and the highest MFI. The dynamics of hfRPE and 1F-iPS–RPE are quite similar, although the percentage of phagocytosis in 1F-iPS–RPE cells is higher (Fig. 4B). Since $\alpha_v\beta_5$ integrin receptor density is highest in ARPE-19 and 1F-iPS-RPE, these data suggest that $\alpha_v\beta_5$ integrin expression may have the greatest impact on the rate of phagocytosis compared with CD36 and MerTK. Since the 1F-iPS–RPE phagocytosis rates were more efficient in this experiment (Fig. 4B compared with Fig. 3C), we hypothesized that differentiation status may also be important since several weeks had passed between experiments. To test this idea, we examined the receptor density of the phagocytosis receptors and phagocytosis dynamics of a cell line that we recently generated (EiPS-RPE)[18] at distinct time points. As the RPE cells became more heavily pigmented and developed more typical hexagonal morphologies (Fig. 5A–C), dynamic surface receptor remodeling occurred (Fig. 5D), and the RPE cells became more efficient at phagocytosing POS (Fig. 5E). Therefore, we conclude that as RPE cells in culture become more differen-

tiated, the receptor density of the phagocytosis receptors changes in a fashion that favors more efficient POS phagocytosis.

## Conclusions

The ability of RPE cells to phagocytose POS is critical to their function. We have developed a flow cytometry–based method to assess phagocytic activity in cultured RPE and iPSC-derived RPE. This method allows for the determination of both binding and internalization of POS by these cell types. These measures are useful for characterizing RPE cells and to provide educated estimations about how well they may function in vivo. In this study, we examined the expression of cell surface receptors known to be involved in POS phagocytosis in an attempt to explain the differences observed in the phagocytic activities of different RPE cell types. Since 10,000+ cells are analyzed per condition, robust and unbiased quantification can be performed using this technique and variation is reduced to negligible levels.

We have previously demonstrated that 1F-iPS–RPE derived using directed differentiation closely resemble hfRPE in multiple assays (histologic, proteomic, and metabolomic).[14] The key finding from the current project is that 1F-iPS–RPE also closely resemble hfRPE based on expression and density of key receptors involved in RPE phagocytosis. 1F-iPS–RPE, EiPS-RPE, and primary human RPE also display similar dynamics of POS binding and internalization. Few similarities are observed, however, with ARPE-19. Based on our results, of the four human cell lines compared, ARPE-19 cells display faster kinetics of binding and internalization. This may be due to marked differences in $\alpha_v\beta_5$ integrin and/or CD36 receptor expression and density (and perhaps cellular morphology). Both of these receptors are expressed at much higher levels than detected on hfRPE or 1F-iPS–RPE cells. The expression and density of MerTK is very similar in ARPE-19 and 1F-iPS–RPE, but highest in hfRPE. Somewhat paradoxically, in this assay hfRPE have the lowest percentage of internalization and MFI of the cell types compared. These data may suggest that $\alpha_v\beta_5$ integrin expression and density dictates the rate of phagocytosis. This argument is supported by the demonstration that higher $\alpha_v\beta_5$ integrin expression (and lower MerTK) is observed in 1F-iPS–RPE compared with hfRPE, but 1F-iPS–RPE display higher percentages of phagocytosis, meaning more cells are able to bind and phagocytose POS. In addition, over expression of $\alpha_v\beta_5$ integrin induces a very dramatic change to the phagocytosis ability of ARPE-19 cells. One hundred percent of cells transfected with $\alpha_v\beta_5$ integrin phagocytose POS at greater numbers than cells transfected with CD36, MerTK, or especially GFP. Lastly, during differentiation $\alpha_v\beta_5$ integrin levels steadily increase correlating with improved phagocytic dynamics. This outcome is not surprising based on previously reporting findings suggesting that $\alpha_v\beta_5$ integrins are the primary binding receptors for POS[19] and may function upstream of MerTK to initiate internalization.[33] In this study, we report that dynamic remodeling of the surface phagocytosis receptors occurs in iPS-RPE cells during differentiation; these differences affect the binding and internalization dynamics. Since this assay is simple and quick, it may be performed at various time points to determine the optimal time for implantation in human patients once optimal phagocytosis dynamics are observed in vitro.

We present evidence in this study that iPS-RPE phagocytose POS at similar rates as primary human RPE and this is a highly desirable outcome, since the use of these cells is being explored in transplantation studies for therapeutic intervention of AMD, a disease for which no cure has been discovered.[2,3] It is also encouraging that iPS-RPE cells do not closely resemble ARPE-19 cells based on these analyses. ARPE-19 cells are immortalized and do not resemble primary RPE cells morphologically or in proteomic and metabolomic analyses.[14] Consequently, we offer in this study additional evidence that iPS-RPE cells may provide excellent substitutions for diseased RPE in human subjects with AMD or other RPE-mediated retinal degenerations.

### *Acknowledgments*

The authors thank Alison L. Dorsey, BS, and Mandy Lehmann, PhD, for advice and technical assistance. Samples for electron microscopy were prepared and imaged by Malcolm R. Wood, PhD, in the Scripps Research Institute (TSRI) Electron Microscopy core facility. The staff at the TSRI flow cytometry core facility also provided expert help.

### *References*

1. Strauss O. The retinal pigment epithelium in visual function. *Physiol Rev*. 2005;85:845–881.
2. Congdon N, O'Colmain B, Klaver CC, et al. Causes and prevalence of visual impairment among adults in the United States. *Arch Ophthalmol*. 2004;122:477–485.
3. Resnikoff S, Pascolini D, Etya'ale D, et al. Global data on visual impairment in the year 2002. *Bull World Health Organ*. 2004; 82:844–851.
4. Bok D, Hall MO. The role of the pigment epithelium in the etiology of inherited retinal dystrophy in the rat. *J Cell Biol*. 1971;49:664–682.
5. Charbel Issa P, Bolz HJ, Ebermann I, et al. Characterisation of severe rod-cone dystrophy in a consanguineous family with a splice site mutation in the MERTK gene. *Br J Ophthalmol*. 2009;93:920–925.
6. D'Cruz PM, Yasumura D, Weir J, et al. Mutation of the receptor tyrosine kinase gene Mertk in the retinal dystrophic RCS rat. *Hum Mol Genet*. 2000;9:645–651.
7. Takahashi K, Tanabe K, Ohnuki M, et al. Induction of pluripotent stem cells from adult human fibroblasts by defined factors. *Cell*. 2007;131:861–872.
8. Yu J, Vodyanik MA, Smuga-Otto K, et al. Induced pluripotent stem cell lines derived from human somatic cells. *Science*. 2007;318:1917–1920.
9. Buchholz DE, Hikita ST, Rowland TJ, et al. Derivation of functional retinal pigmented epithelium from induced pluripotent stem cells. *Stem Cells*. 2009;27:2427–2434.
10. Carr AJ, Vugler AA, Hikita ST, et al. Protective effects of human iPS-derived retinal pigment epithelium cell transplantation in the retinal dystrophic rat. *PLoS One*. 2009;4:e8152.
11. Hirami Y, Osakada F, Takahashi K, et al. Generation of retinal cells from mouse and human induced pluripotent stem cells. *Neurosci Lett*. 2009;458:126–131.
12. Meyer JS, Shearer RL, Capowski EE, et al. Modeling early retinal development with human embryonic and induced pluripotent stem cells. *Proc Natl Acad Sci U S A*. 2009;106: 16698–16703.
13. Osakada F, Jin ZB, Hirami Y, et al. In vitro differentiation of retinal cells from human pluripotent stem cells by small-molecule induction. *J Cell Sci*. 2009;122:3169–3179.
14. Krohne T, Westenskow PD, Kurihara T, et al. Generation of retinal pigment epithelial cells from small molecules and OCT-reprogrammed human induced pluripotent stem cells. *Stem Cells Transl Med*. 2012;1:96–109.
15. Idelson M, Alper R, Obolensky A, et al. Directed differentiation of human embryonic stem cells into functional retinal pigment epithelium cells. *Cell Stem Cell*. 2009;5:396–408.

16. Vugler A, Carr AJ, Lawrence J, et al. Elucidating the phenomenon of HESC-derived RPE: anatomy of cell genesis, expansion and retinal transplantation. *Exp Neurol*. 2008;214:347–361.
17. Zhu S, Li W, Zhou H, et al. Reprogramming of human primary somatic cells by OCT4 and chemical compounds. *Cell Stem Cell*. 2010;7:651–655.
18. Zhao T, Zhang ZN, Rong Z, Xu Y. Immunogenicity of induced pluripotent stem cells. *Nature*. 2011;474:212–215.
19. Finnemann SC, Bonilha VL, Marmorstein AD, Rodriguez-Boulan E. Phagocytosis of rod outer segments by retinal pigment epithelial cells requires αvβ5 integrin for binding but not for internalization. *Proc Natl Acad Sci U S A*. 1997;94:12932–12937.
20. Lin H, Clegg DO. Integrin alphavbeta5 participates in the binding of photoreceptor rod outer segments during phagocytosis by cultured human retinal pigment epithelium. *Invest Ophthalmol Vis Sci*. 1998;39:1703–1712.
21. Miceli MV, Newsome DA, Tate DJ Jr. Vitronectin is responsible for serum-stimulated uptake of rod outer segments by cultured retinal pigment epithelial cells. *Invest Ophthalmol Vis Sci*. 1997;38:1588–1597.
22. Ryeom SW, Sparrow JR, Silverstein RL. CD36 participates in the phagocytosis of rod outer segments by retinal pigment epithelium. *J Cell Sci*. 1996;109:387–395.
23. Nandrot EF, Kim Y, Brodie SE, Huang X, Sheppard D, Finnemann SC. Loss of synchronized retinal phagocytosis and age-related blindness in mice lacking alphavbeta5 integrin. *J Exp Med*. 2004;200:1539–1545.
24. Finnemann SC, Silverstein RL. Differential roles of CD36 and alphavbeta5 integrin in photoreceptor phagocytosis by the retinal pigment epithelium. *J Exp Med*. 2001;194:1289–1298.
25. Houssier M, Raoul W, Lavalette S, et al. CD36 deficiency leads to choroidal involution via COX2 down-regulation in rodents. *PLoS Med*. 2008;5:e39.
26. Chang Y, Finnemann SC. Tetraspanin CD81 is required for the αvβ5-integrin-dependent particle-binding step of RPE phagocytosis. *J Cell Sci*. 2007;120:3053–3063.
27. Boyle D, Tien LF, Cooper NG, Shepherd V, McLaughlin BJ. A mannose receptor is involved in retinal phagocytosis. *Invest Ophthalmol Vis Sci*. 1991;32:1464–1470.
28. Lu PD, Harding HP, Ron D. Translation reinitiation at alternative open reading frames regulates gene expression in an integrated stress response. *J Cell Biol*. 2004;167:27–33.
29. Wu Y, Singh S, Georgescu MM, Birge RB. A role for Mer tyrosine kinase in alphavbeta5 integrin-mediated phagocytosis of apoptotic cells. *J Cell Sci*. 2005;118:539–553.
30. Kennedy CJ, Rakoczy PE, Constable IJ. A simple flow cytometric technique to quantify rod outer segment phagocytosis in cultured retinal pigment epithelial cells. *Curr Eye Res*. 1996;15:998–1003.
31. Karl MO, Valtink M, Bednarz J, Engelmann K. Cell culture conditions affect RPE phagocytic function. *Graefes Arch Clin Exp Ophthalmol*. 2007;245:981–991.
32. Miceli MV, Newsome DA. Insulin stimulation of retinal outer segment uptake by cultured human retinal pigment epithelial cells determined by a flow cytometric method. *Exp Eye Res*. 1994;59:271–280.
33. Finnemann SC. Focal adhesion kinase signaling promotes phagocytosis of integrin-bound photoreceptors. *EMBO J*. 2003;22:4143–4154.